Turkish **J**ournal of **M**athematics and **C**omputer **S**cience
TJMCS

http://tjmcs.matder.org.tr/

@TJMCS
© MatDer
http://www.matder.org.tr/

Numerical Investigation of a Steady Flow of an Incompressible Fluid in a Lid Driven Cavity

Hüseyin Demir and Serpil Şahin

Abstract. In this paper, numerical investigation for 2-D steady-state, incompressible pseudoplastic viscous flow is presented. Pseudo time derivative is used to solve the continuity and momentum equations with suitable boundary conditions. Depending on high Reynolds number, wall motions of flow are investigated with respect to nonlinear viscosity by using Cross model. This study has been undertaken as a first step toward understanding in heat and mass transport in solvent and polymer processing equipment. Solution to the vorticity equation for moving top wall is obtained numerically and found to be stable and convergent for high value of Reynolds numbers. In fact some new results, which are governed by inertia and variable shear-rate, are obtained and then this has been documented first time.

2010 AMS Classification: 76A05, 76D05

Keywords: 2-D steady-state, Incompressible pseudoplastic viscous flow, Pseudo-time derivative, High Reynolds number.

1. INTRODUCTION

Numerical methods are frequently used for two dimensional steady incompressible Newtonian and non-Newtonian flow problems. Due to the simplicity of cavity geometry, numerical methods can be applied very easily and effectively to this type of flow problems and the results are very satisfactory. Despite the simplicity of this geometry, there is a rich flow on the corners of cavity depending on Reynolds number. There are many available different numerical methods applied to this flow problem in the literature. Though it has been studied by many researchers extensively, there are still some points of concern to be clarified. For example;

(1) Many different numerical methods for the solution of cavity flow problem gives similar results as $\mathrm{Re} \leq 1000$. But the solutions deviate from each other as Reynolds number gets higher.
(2) In some studies, steady solutions obtained even for high Reynolds number.

For such studies, Benjamin and Denny [3] have used a method which is relaxed by means of ADI methods using a non-uniform iteration parameter. Full converged solutions at Reynolds number up to 10^4 with three different grid mesh sizes (maximum being 101×101) are generated in order to resolve basic questions on the nature of the flow and to explore convergence properties of the method.

Rubin and Khosla [13] have used the strongly implicit numerical method with 2×2 coupled stream function-vorticity form of the Navier -Stokes equations. They have obtained solutions at Reynolds number up to 3000 with a grid mesh of 17×17.

Schreiber and Keller [14] have introduced efficient and reliable numerical techniques of high-order accuracy for solving problems of steady viscous incompressible flow in the plane, and are used to obtain accurate solutions for the driven cavity. The numerical methods combine an efficient linear system solver, an adaptive Newton-like method for nonlinear systems. They have obtained solutions at Reynolds number 10000 on a 180×180.

Gupta [9] has used a fourth $\left(\Delta h^4\right)$ order compact scheme for the numerical solution of the driven cavity flow. Then he has used a 9 point to approximate for the stream function and vorticity equations up to fourth order accuracy. He has presented steady cavity flow solutions for $\mathrm{Re} \leq 2000$ with a maximum of 41×41 grid mesh by using SOR iteration method.

Li et. al. [11] have used a fourth $\left(\Delta h^4\right)$ order compact scheme which had a faster convergence than that of Gupta [9]. They have solved the cavity flow with a grid size of 129×129 for $\mathrm{Re} \leq 7500$.

Hou et. al. [10] have used Lattice Boltzmann Method for simulation of the cavity flow. They have used 256×256 grid point and presented solutions for Reynolds number $\mathrm{Re} \leq 7500$.

Liao and Zhu [12] have used a higher order stream function-vorticity boundary element method (BEM) formulation for the solution of Navier-Stokes equations. With this they have presented solutions up to $\mathrm{Re} = 10000$ with a grid mesh of 257×257.

Goyon [8] has solved the stream function-vorticity equations using Incremental unknowns. He has presented steady solutions for $\mathrm{Re} \leq 7500$ on a maximum grid size of 256×256

Demir [5] has investigated the stability properties of wall motions in a cavity region. Depending on high Reynolds number, he has studied both steady-state and time dependent viscous as well as viscoelastic flow with Gauss-Seidel, SOR and ADI (Peaceman-Rachford) methods, respectively.

Recently, Barragy and Carey [1] have used a p-type finite element scheme on a 257×257 strongly graded and refined element mesh. They have obtained highly accurate $\left(\Delta h^8\right)$ solutions for steady cavity flow solutions for $\mathrm{Re} \leq 12500$.

On the other hand, Botella and Peyret [4] have used a Chebyshev collocation method for the solution of wall driven cavity flow. They have obtained a highly accurate spectral solutions for the cavity flow with a maximum of grid mesh of $N = 160$ (polynomial degree) for Reynolds number $\mathrm{Re} \leq 9000$. They concluded that their numerical solutions exhibit a periodic behavior beyond this Re.

Erturk, Corke and Gokcol [6] have introduced an effective numerical method for driven cavity flow by using stream function and vorticity formulation. Using regular

grid size of 601×601 and they solved the Navier-Stokes equations for high Reynolds number $\mathrm{Re} \leq 21000$.

As known many factors effect the accuracy of a numerical solution, such as, the number of grids, the spatial discretization order of the finite difference equations and also the boundary conditions used in the solution. Also it is well known that as the number of grids is increased a numerical solution gets more accurate. Therefore in this study the effect of number of grid points in a mesh on the accuracy of the numerical solution wall driven cavity flow is investigated, especially as the Reynolds number increases. For this, 2-D steady-state, incompressible pseudoplastic viscous flow equations are solved on progressively increasing number of grid points (from 128×128 to 401×401).

2. NUMERICAL METHOD

The following figures schematically represent the flow in a lid driven cavity region.

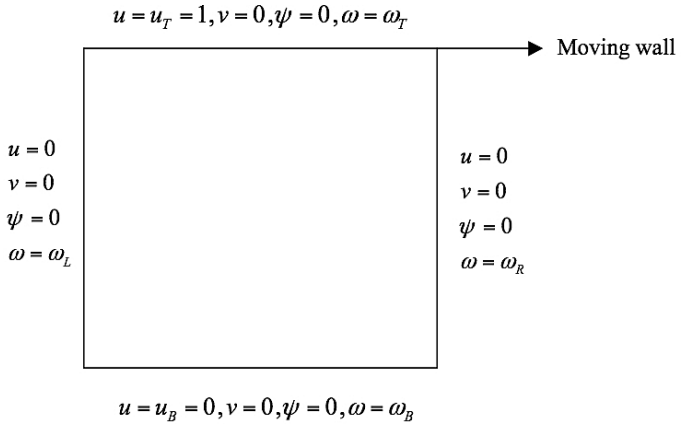

FIGURE 1. Physical configuration and description of boundary condition.

We use the stream function (ψ) and vorticity (ω) formulation for the lid-driven flow of the steady-state incompressible pseudoplastic viscous fluid equations in the form:

$$\frac{\partial^2 \psi}{\partial x^2} + \frac{\partial^2 \psi}{\partial y^2} = -\omega \tag{2.1}$$

$$\begin{aligned} u\frac{\partial \omega}{\partial x} + v\frac{\partial \omega}{\partial y} =& \frac{1}{\mathrm{Re}\eta(q)} \left\{ \frac{\partial}{\partial x}\left(\eta^2(q)\frac{\partial \omega}{\partial x}\right) + \frac{\partial}{\partial y}\left(\eta^2(q)\frac{\partial \omega}{\partial y}\right) \right\} \\ &+ \frac{1}{\mathrm{Re}} \left\{ -4\frac{\partial^2 \psi}{\partial x \partial y}\frac{\partial^2 \eta(q)}{\partial x \partial y} - \left(\frac{\partial^2 \psi}{\partial y^2} - \frac{\partial^2 \psi}{\partial x^2}\right)\left(\frac{\partial^2 \eta(q)}{\partial y^2} - \frac{\partial^2 \eta(q)}{\partial x^2}\right) \right\} \end{aligned} \tag{2.2}$$

$$u = \frac{\partial \psi}{\partial y}, \quad v = -\frac{\partial \psi}{\partial x} \tag{2.3}$$

where, Re is the Reynolds number, q is the shear rate, $\eta(q)$ is the viscosity, and x and y are the Cartesian coordinates as shown in Figure 1. Finally, the Cross model is used in this work for modeling of the viscosity function and this is known as

$$\eta\left(q\right)=\eta\left(\infty\right)+\frac{\left(\eta\left(0\right)-\eta\left(\infty\right)\right)}{1+\left(\lambda q\right)^{1-n}}$$

In this Cross Model, $\eta(\infty)$ represents the infinite shear viscosity for very large deformation rates and $\eta(0)$ represents the zero shear rate viscosity for very small rates of shear. Assuming $n=0.5\,,\lambda=1\,,\eta(0)=1$ and $0\leq\eta(\infty)\leq 1$, we obtain shear-thinning or so-called pseudoplastic behavior.

The first order pseudo time derivatives are now introduced into equations (2.1) and (2.2) follows:

$$\frac{\partial\psi}{\partial t}=\frac{\partial^2\psi}{\partial x^2}+\frac{\partial^2\psi}{\partial y^2}+\omega \tag{2.4}$$

$$\begin{aligned}\frac{\partial\omega}{\partial t}=&-\frac{\partial\psi}{\partial y}\frac{\partial\omega}{\partial x}+\frac{\partial\psi}{\partial x}\frac{\partial\omega}{\partial y}+\frac{1}{\mathrm{Re}\eta(q)}\left\{\frac{\partial}{\partial x}\left(\eta^2(q)\frac{\partial\omega}{\partial x}\right)+\frac{\partial}{\partial y}\left(\eta^2(q)\frac{\partial\omega}{\partial y}\right)\right\}\\&+\frac{1}{\mathrm{Re}}\left\{-4\frac{\partial^2\psi}{\partial x\partial y}\frac{\partial^2\eta(q)}{\partial x\partial y}-\left(\frac{\partial^2\psi}{\partial y^2}-\frac{\partial^2\psi}{\partial x^2}\right)\left(\frac{\partial^2\eta(q)}{\partial y^2}-\frac{\partial^2\eta(q)}{\partial x^2}\right)\right\}\end{aligned} \tag{2.5}$$

Using forward difference approximation for the time derivatives in equations (2.4) and (2.5), we get on rearrangement the following equations:

$$\left(1-\Delta t\frac{\partial^2}{\partial x^2}-\Delta t\frac{\partial^2}{\partial y^2}\right)\psi^{n+1}=\psi^n+\Delta t\omega^n \tag{2.6}$$

$$\begin{aligned}&\left[1-\Delta t\frac{\partial\psi^n}{\partial x}\frac{\partial}{\partial y}+\Delta t\frac{\partial\psi^n}{\partial y}\frac{\partial}{\partial x}-\frac{\Delta t}{\mathrm{Re}}\eta^n\frac{\partial^2}{\partial x^2}\right.\\&\left.-2\frac{\Delta t}{\mathrm{Re}}\frac{\partial\eta^n}{\partial x}\frac{\partial}{\partial x}-\frac{\Delta t}{\mathrm{Re}}\eta^n\frac{\partial^2}{\partial y^2}-2\frac{\Delta t}{\mathrm{Re}}\frac{\partial\eta^n}{\partial y}\frac{\partial}{\partial y}\right]\omega^{n+1}=\omega^n\\&+\frac{\Delta t}{\mathrm{Re}}\left\{-4\frac{\partial^2\psi^n}{\partial x\partial y}\frac{\partial^2\eta^n}{\partial x\partial y}-\left(\frac{\partial^2\psi^n}{\partial y^2}-\frac{\partial^2\psi^n}{\partial x^2}\right)\left(\frac{\partial^2\eta^n}{\partial y^2}-\frac{\partial^2\eta^n}{\partial x^2}\right)\right\}\end{aligned} \tag{2.7}$$

Noting that Δt is quite small, we now spatially factorize equations (2.6) and (2.7) as follows:

$$\left(1-\Delta t\frac{\partial^2}{\partial x^2}\right)\left(1-\Delta t\frac{\partial^2}{\partial y^2}\right)\psi^{n+1}=\psi^n+\Delta t\omega^n \tag{2.8}$$

(2.9)

$$\begin{aligned}&\left(1-\frac{\Delta t}{\mathrm{Re}}\eta^n\frac{\partial^2}{\partial x^2}+\Delta t\left(\frac{\partial\psi}{\partial y}\right)^n\frac{\partial}{\partial x}-2\frac{\Delta t}{\mathrm{Re}}\left(\frac{\partial\eta}{\partial x}\right)^n\frac{\partial}{\partial x}\right)\left(1-\frac{\Delta t}{\mathrm{Re}}\eta^n\frac{\partial^2}{\partial y^2}-\Delta t\left(\frac{\partial\psi}{\partial x}\right)^n\frac{\partial}{\partial y}\right.\\&\left.-2\frac{\Delta t}{\mathrm{Re}}\left(\frac{\partial\eta}{\partial y}\right)^n\frac{\partial}{\partial y}\right)\omega^{n+1}=\omega^n+\frac{\Delta t}{\mathrm{Re}}\left\{-4\left(\frac{\partial^2\psi}{\partial x\partial y}\right)^n\left(\frac{\partial^2\eta}{\partial x\partial y}\right)^n-\left[\left(\frac{\partial^2\psi}{\partial y^2}\right)^n-\left(\frac{\partial^2\psi}{\partial x^2}\right)^n\right]\right.\\&\left.\times\left[\left(\frac{\partial^2\eta}{\partial y^2}\right)^n-\left(\frac{\partial^2\eta}{\partial x^2}\right)^n\right]\right\}\end{aligned}$$

In the event of reaching a steady state, we have

$$\psi^{n+1} = \psi^n \tag{2.10}$$

and

$$\omega^{n+1} = \omega^n \tag{2.11}$$

Using this result in the right hand side of equations (2.10) and (2.11), we may write

$$\left(1-\Delta t\frac{\partial^2}{\partial x^2}\right)\left(1-\Delta t\frac{\partial^2}{\partial y^2}\right)\psi^{n+1} = \psi^n + \Delta t\omega^n + \left(\Delta t\frac{\partial^2}{\partial x^2}\right)\left(\Delta t\frac{\partial^2}{\partial y^2}\right)\psi^n \tag{2.12}$$

$$\begin{aligned}
&\left(1-\frac{\Delta t}{\mathrm{Re}}\eta^n\frac{\partial^2}{\partial x^2}+\Delta t\left(\frac{\partial\psi}{\partial y}\right)^n\frac{\partial}{\partial x}-2\frac{\Delta t}{\mathrm{Re}}\left(\frac{\partial\eta}{\partial x}\right)^n\frac{\partial}{\partial x}\right)\left(1-\frac{\Delta t}{\mathrm{Re}}\eta^n\frac{\partial^2}{\partial y^2}-\Delta t\left(\frac{\partial\psi}{\partial x}\right)^n\frac{\partial}{\partial y}\right.\\
&\left.-2\frac{\Delta t}{\mathrm{Re}}\left(\frac{\partial\eta}{\partial y}\right)^n\frac{\partial}{\partial y}\right)\omega^{n+1} = \omega^n + \frac{\Delta t}{\mathrm{Re}}\left\{-4\left(\frac{\partial^2\psi}{\partial x\partial y}\right)^n\left(\frac{\partial^2\eta}{\partial x\partial y}\right)^n-\left[\left(\frac{\partial^2\psi}{\partial y^2}\right)^n-\left(\frac{\partial^2\psi}{\partial x^2}\right)^n\right]\right.\\
&\left.\times\left[\left(\frac{\partial^2\eta}{\partial y^2}\right)^n-\left(\frac{\partial^2\eta}{\partial x^2}\right)^n\right]\right\}+\left(-\frac{\Delta t}{\mathrm{Re}}\eta^n\frac{\partial^2}{\partial x^2}+\Delta t\left(\frac{\partial\psi}{\partial y}\right)^n\frac{\partial}{\partial x}-2\frac{\Delta t}{\mathrm{Re}}\left(\frac{\partial\eta}{\partial x}\right)^n\frac{\partial}{\partial x}\right)\\
&\times\left(-\frac{\Delta t}{\mathrm{Re}}\eta^n\frac{\partial^2}{\partial y^2}-\Delta t\left(\frac{\partial\psi}{\partial x}\right)^n\frac{\partial}{\partial y}-2\frac{\Delta t}{\mathrm{Re}}\left(\frac{\partial\eta}{\partial y}\right)^n\frac{\partial}{\partial y}\right)\omega^n
\end{aligned} \tag{2.13}$$

The solution method for the equations (2.12) and (2.13) involves a two-level updating. First the stream function equation is solved. For equation (2.12) the variable f is introduced such that

$$\left(1-\Delta t\frac{\partial^2}{\partial y^2}\right)\psi^{n+1} = f \tag{2.14}$$

and

$$\left(1-\Delta t\frac{\partial^2}{\partial x^2}\right)f = \psi^n + \Delta t\omega^n + \left(\Delta t\frac{\partial^2}{\partial x^2}\right)\left(\Delta t\frac{\partial^2}{\partial y^2}\right)\psi^n \tag{2.15}$$

In equation (2.15), f is the only unknown and this equation is first solved at each grid point. Following this, the stream function variable (ψ) is advanced into the new time level using equation (2.14). Next the vorticity equation is solved in a similar fashion.

3. RESULTS AND DISCUSSION

We use the symmetry for ψ and ω at spurious points outside the boundaries. On the boundaries the values of vorticity are chosen from the nine-point compact finite difference.

Left Boundary	Right Boundary
$\psi_{-1,j} = \psi_{1,j}\ ,\ \psi_{0,j} = 0$	$\psi_{N+1,j} = \psi_{N-1,j}\ ,\ \psi_{N,j} = 0$
$\omega_{0,j} = -\left(\frac{\partial^2\psi}{\partial x^2}\right)_{0,j}$	$\omega_{N,j} = -\left(\frac{\partial^2\psi}{\partial x^2}\right)_{N,j}$

Bottom Boundary	Top Boundary
$\psi_{i,-1} = \psi_{i,1}\,,\ \psi_{i,0} = 0$	$\psi_{i,N+1} = \psi_{i,N-1}\,,\ \psi_{i,N} = 0$
$\omega_{i,0} = -\left(\dfrac{\partial^2 \psi}{\partial y^2}\right)_{i,0}$	$\omega_{i,N} = -\left(\dfrac{\partial^2 \psi}{\partial y^2}\right)_{i,N}$

During our computations we monitored the residual of the steady streamfunction and vorticity equations (2.1) and (2.2) as a measure of the convergence to the steady state solution, where the residual of each equation is given as

$$R_\psi = \frac{\psi_{i-1,j}^{n+1} - 2\psi_{i,j}^{n+1} + \psi_{i+1,j}^{n+1}}{\Delta x^2} + \frac{\psi_{i,j-1}^{n+1} - 2\psi_{i,j}^{n+1} + \psi_{i,j+1}^{n+1}}{\Delta y^2} + \omega_{i,j}^{n+1} \tag{3.16}$$

(3.17)

$$\begin{aligned}
R_\omega = {} & \frac{1}{\mathrm{Re}}\eta_{i,j}^{n+1}\frac{\omega_{i-1,j}^{n+1} - 2\omega_{i,j}^{n+1} + \omega_{i+1,j}^{n+1}}{\Delta x^2} + \frac{2}{\mathrm{Re}}\frac{\eta_{i+1,j}^{n+1} - \eta_{i-1,j}^{n+1}}{2\Delta x}\frac{\omega_{i+1,j}^{n+1} - \omega_{i-1,j}^{n+1}}{2\Delta x} \\
& + \frac{1}{\mathrm{Re}}\eta_{i,j}^{n+1}\frac{\omega_{i,j-1}^{n+1} - 2\omega_{i,j}^{n+1} + \omega_{i,j+1}^{n+1}}{\Delta y^2} + \frac{2}{\mathrm{Re}}\frac{\eta_{i,j+1}^{n+1} - \eta_{i,j-1}^{n+1}}{2\Delta y}\frac{\omega_{i,j+1}^{n+1} - \omega_{i,j-1}^{n+1}}{2\Delta y} \\
& - \frac{4}{\mathrm{Re}}\frac{\psi_{i+1,j+1}^{n+1} - \psi_{i-1,j+1}^{n+1} - \psi_{i+1,j-1}^{n+1} + \psi_{i-1,j-1}^{n+1}}{4\Delta x\Delta y}\frac{\eta_{i+1,j+1}^{n+1} - \eta_{i-1,j+1}^{n+1} - \eta_{i+1,j-1}^{n+1} + \eta_{i-1,j-1}^{n+1}}{4\Delta x\Delta y} \\
& - \frac{1}{\mathrm{Re}}\left(\frac{\psi_{i,j-1}^{n+1} - 2\psi_{i,j}^{n+1} + \psi_{i,j+1}^{n+1}}{\Delta y^2} - \frac{\psi_{i-1,j}^{n+1} - 2\psi_{i,j}^{n+1} + \psi_{i+1,j}^{n+1}}{\Delta x^2}\right) \\
& \times \left(\frac{\eta_{i,j-1}^{n+1} - 2\eta_{i,j}^{n+1} + \eta_{i,j+1}^{n+1}}{\Delta y^2} - \frac{\eta_{i-1,j}^{n+1} - 2\eta_{i,j}^{n+1} + \eta_{i+1,j}^{n+1}}{\Delta x^2}\right) - \frac{\psi_{i,j+1}^{n+1} - \psi_{i,j-1}^{n+1}}{2\Delta y}\frac{\omega_{i+1,j}^{n+1} - \omega_{i-1,j}^{n+1}}{2\Delta x} \\
& + \frac{\psi_{i+1,j}^{n+1} - \psi_{i-1,j}^{n+1}}{2\Delta x}\frac{\omega_{i,j+1}^{n+1} - \omega_{i,j-1}^{n+1}}{2\Delta y}
\end{aligned}$$

We use to solve the partial differential equation numerically is always consistent and stable. It is consistent because the truncation error tends to zero and it is stable because of diagonal dominance. In our computations, for all Reynolds numbers, we have considered that convergence is achieved when for each Equations (3.16) and (3.17) the maximum of the absolute residual in the computational domain ($\max(|R_\psi|)$ and $\max(|R_\omega|)$) are less than 10^{-4} . Such a low value is chosen to ensure the accuracy of the solution. At these residual levels, the maximum absolute difference in vorticity function value between two time steps, $\left(\max\left(\left|\omega^{n+1} - \omega^n\right|\right)\right)$, is in order of 10^{-8} and for stream function, $\left(\max\left(\left|\psi^{n+1} - \psi^n\right|\right)\right)$,is in order of 10^{-10}. And also at these convergence levels, between two time steps the maximum absolute normalized difference in vorticity function, $\left(\max\left(\left|\frac{\omega^{n+1} - \omega^n}{\omega^n}\right|\right)\right)$, and in stream function, $\left(\max\left(\left|\frac{\psi^{n+1} - \psi^n}{\psi^n}\right|\right)\right)$, are in order of 10^{-5}, and 10^{-10} respectively.

Reference	Grid	ψ	ω	x	y
Erturk et al. [6], 2005	401×401	0.118585	2.062761	0.5300	0.5650
	513×513	0.118722	2.064765	0.5313	0.5645
	601×601	0.118781	2.065530	0.5300	0.5650
Schreiber and	121×121	0.11492	2.0112	-	-
Keller[[14], 1983	141×141	0.11603	2.0268	0.52857	0.56429
Ghia et al. [7], 1982	129×129	0.117929	2.04968	0.5313	0.5625
Hou et al. [10],1995	256×256	0.1178	2.0760	0.5333	0.5647
Liao et al. [12], 1996	129×129	0.1160	2.0234	0.5313	0.5625
Benjamin et al. [3],1979	101×101	0.1175	2.044	-	-
Present	128×128	0.115952	2.02482	0.5313	0.5625
	256×256	0.118182	2.05677	0.5313	0.5664
	401×401	0.118626	2.06322	0.5312	0.5661

TABLE 1. Comparison of the properties of the primary vortex; the maximum stream function value, the vorticity value and the location of the centre, for Newtonian fluid at Re = 1000.

Table 1 tabulates the maximum stream function value, the vorticity value at the centre of the primary vortex and also the centre location of the primary vortex for Newtonian fluid at Re = 1000 along with similar results found in the literature are compared. In Table 1 among the most significant results, Erturk, Corke and Gokcol [6] have solved the cavity flow on three different grid mesh (401×401 , 513×513 , 601×601) for Re = 1000.

Looking back to Table 1, for Re = 1000, our results are in very good agreement with the results of Schreiber and Keller [14], Hou et al. [10], and Erturk et al. [6]. From all these comparisons we can conclude that even for Re = 1000 higher order approximations together with the use of fine grids are necessary for accuracy.

Re	Grid	ψ	ω	x	y
	128×128	0.095881	1.563308	0.5313	0.5391
1000	256×256	0.104641	1.690638	0.5273	0.5391
	401×401	0.106355	1.715892	0.5262	0.5411
	128×128	0.102999	1.621777	0.5234	0.5313
2000	256×256	0.102640	1.616420	0.5195	0.5313
	401×401	0.106473	1.673982	0.5187	0.5312

TABLE 2. The maximum stream function value, the vorticity value and the location of the center, for viscous pseudoplastic fluid at Re = 1000 and Re = 2000.

Table 2 tabulates the maximum stream function value, the vorticity value at the center of the primary vortex and also the center location of the primary vortex for viscous pseudoplastic fluid at Re = 1000 and Re = 2000 are introduced. This table has been documented first time and our results are seen in Figure 2, 3 and 4 at Re = 1000 and Re = 2000 that display for interest significant change from the

Newtonian case in this paper which has not given before. These figures exhibit the formation of the counter-rotating secondary vortices which appear as the Reynolds number increases.

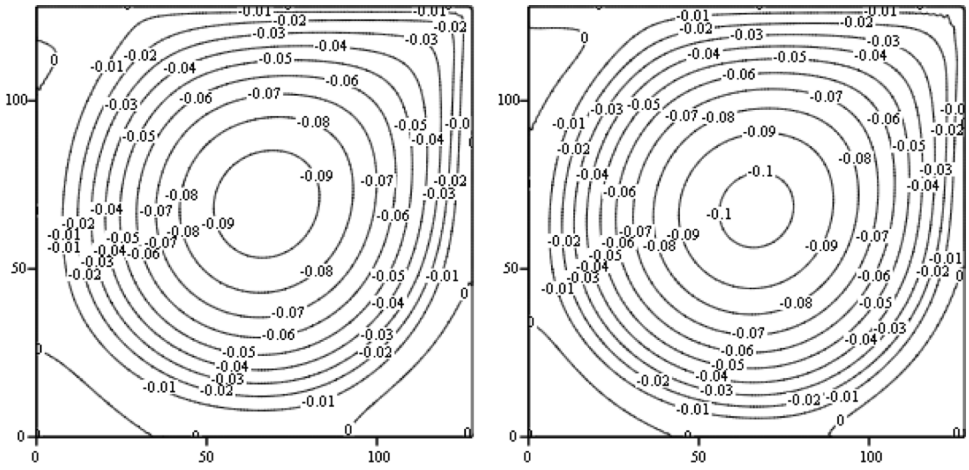

FIGURE 2. Streamline contours of lid-driven cavity flow for $N = 128$ at $Re = 1000$ and $Re = 2000$, respectively .

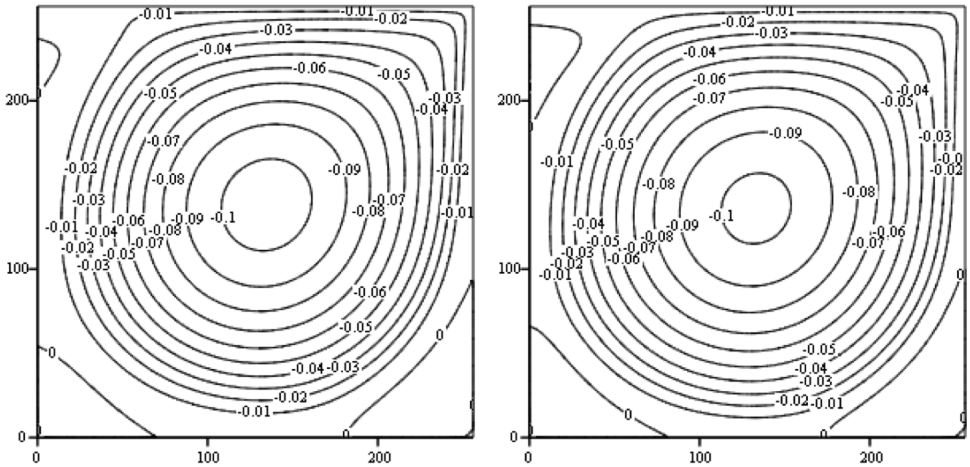

FIGURE 3. Streamline contours of lid-driven cavity flow for $N = 256$ at $Re = 1000$ and $Re = 2000$, respectively .

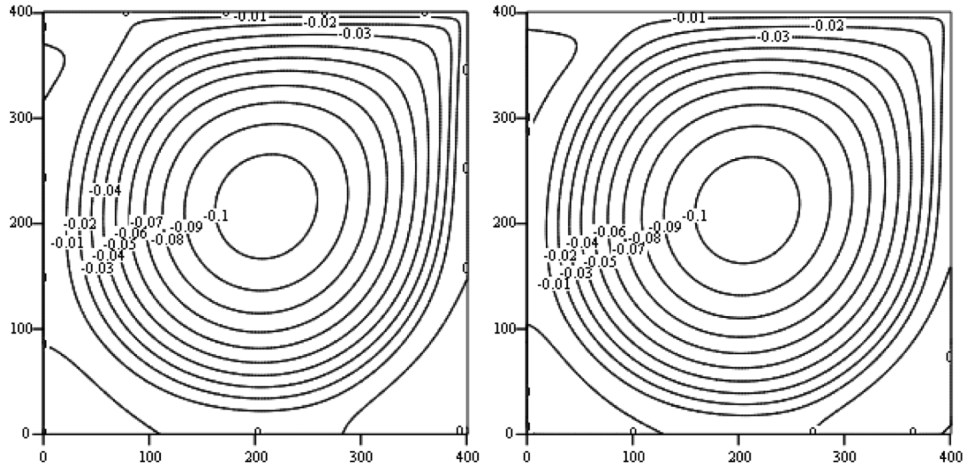

FIGURE 4. Streamline contours of lid-driven cavity flow for $N = 401$ at $Re = 1000$ and $Re = 2000$, respectively .

4. CONCLUSIONS

Numerical solutions of the 2-D steady-state, incompressible pseudoplastic viscous flow for Reynolds numbers up to Re = 2000 have been presented and documented first time. The flow equations in stream function and vorticity formulation are solved computationally using the numerical method described. The stream function and vorticity equations are solved separately by using pseudo time derivative. For each equation, the numerical formulation requires the solution of two tridiagonal systems, which allows the use of large grid meshes easily and we have used a fine grid mesh of 401×401. The numerical solutions converged to maximum absolute residuals of the governing equations that were less than 10^{-4} at all Reynolds number.

REFERENCES

[1] E. Barragy, G.F. Carey. Stream function-vorticity driven cavity solutions using p finite elements. *Computers and Fluids*, 26, 453-468,(1997).

[2] R.M.Beam, R.F.Warming. An implicit factored scheme for the compressible N-S equations. AIAA J., 16, 393-420,(1978).

[3] A.S.Benjamin, V.E.Denny. On the convergence of numerical solutions for 2-D flows in a cavity at large *Re. J. Comp. Physics*, 33, 340-358,(1979).

[4] O.Botella,R. Peyret. Benchmark spectral results on the lid-driven cavity flow. *Computers and Fluids*, 27, 421-433,(1998).

[5] H.Demir. *The Stability Properties of Some RheologicalFlows*. Ph. D. Thesis, The University of Glamorgan, School of Accounting and Mathematics, Division of Maths and Computing, Glamorgan, 264p,1996.

[6] E.Ertürk, T.C.Corke, C.Gökçöl. Numerical solutions of 2-D steady incompressible driven cavity flow at high Reynolds numbers. *J. Numer. Meth. Fluids*, 48, 747-774,(2005).

[7] U.Ghia, K.N.Ghia, C.T.Shin. High-Re solutions for incompressible flow using the N-S equations and a multigrid method. *J. Comp. Physics*, 48, 387-411,(1982).

[8] O.Goyon. High-Re number solutions of N-S equations using incremental unknowns. *Computer Methods in Applied Mechanics and Engineering* , 130, 319-335,(1996).

[9] M.M.Gupta, M.M. High accuracy solutions of incompressible N-S equations. *J. Comp. Physics*, 93, 343-359,(1991).
[10] S.Hou, Q.Zou, S.Chen, G.Doolen, A.C.Cogley. Simulation of cavity flow by the lattice boltzmann method. *J. Comp. Physics*, 118, 329-347,(1995).
[11] M.Li, T.Tang, B.Fornberg. A compact forth-order finite difference scheme for the steady incompressible N-S equations. *Int. J. Numer. Methods Fluids*, 20, 1137-1151,(1995).
[12] S.J.Liao,J.M. Zhu. A short note on higher-order stream function-vorticity formulation of 2-D steady state N-S equations. *Int. J. Numer. Methods Fluids*, 22, 1-9,(1996).
[13] S.G.Rubin,P.K. Khosla. N-S calculations with a coupled strongly implicit method. *Computers and Fluids*, 9, 163-180,(1981).
[14] R.Schreiber, H.B.Keller. Driven cavity flows by efficient numerical techniques. *J. Comp. Physics*, 49, 310-333,(1983).
[15] J.C. Tennehill,D.A. Anderson,R.H.Pletcher. *Computational Fluid Mechanics and Heat Transfer*. Taylor and Francis, 792p,1997.

Hüseyin Demir (hdemir@omu.edu.tr) –Department of Mathematics, Faculty of Science and Art, Ondokuz Mayıs University, Samsun, Turkey.

Serpil Şahin (serpile@omu.edu.tr)– Department of Mathematics, Faculty of Science and Art, Ondokuz Mayıs University, Samsun, Turkey.